

Article

Analysis of Sustained Release Behavior of Drug-Containing Tablet Prepared by CO₂-Assisted Polymer Compression

Yoshito Wakui and Takafumi Aizawa * 

Research Institute for Chemical Process Technology, National Institute of Advanced Industrial Science and Technology, 4-2-1 Nigatake, Miyagino-ku, Sendai 983-8551, Japan; y-wakui@aist.go.jp

* Correspondence: t.aizawa@aist.go.jp; Tel.: +81-22-237-5211

Received: 22 November 2018; Accepted: 17 December 2018; Published: 18 December 2018



Abstract: A controlled-release system for drug delivery allows the continuous supply of a drug to the target region at a predetermined rate for a specified period of time. Herein, the sustained release behavior of a drug-containing tablet fabricated through CO₂-assisted polymer compression (CAPC) was investigated. CAPC involves placing the drug in the center of a nonwoven fabric, sandwiching this fabric between an integer number of nonwoven fabrics, and applying pressure bonding. An elution test, in which the drug-carrying tablet was immersed in water, showed that sustained-release performance can be controlled by the number of nonwoven fabrics covering the top and bottom of the drug-loaded fabric and compression conditions. A model of sustained drug release was formulated to estimate the effective diffusion coefficient in the porous material. Comparative analysis of the bulk diffusion coefficient revealed that the change in diffusion volume due to change in porosity predominates. The tortuosity of the diffusion path was 3–4, and tended to remain almost constant or increase only slightly when the compression rate was increased. These findings show that sustained drug release can be controlled by incorporating the drug into a nonwoven fabric and using the same raw material to encapsulate it.

Keywords: drug delivery; porous polymer; CO₂-assisted polymer compression; sustained release; diffusion; porosity; tortuosity; methylene blue

1. Introduction

Plastics are used in various applications because of their lightness and strength [1]. The form of the plastic, such as board, bead, and fiber, varies depending on its usage. In addition, porous plastics are used as cushioning, heat insulators, sound-absorbing materials, and filters, among others. Further, a porous material with a through-hole is also used as a support for holding a drug [2]. Methods of manufacturing such porous polymer materials include foam injection molding [3] and molding with supercritical CO₂ followed by foaming [4,5].

There are several plastic molding methods such as injection molding, melt spinning, electrospinning, solidification by mixing main and curing agents, and photo formation. In recent years, 3D printers have also been put to practical use in the creation of plastic structures. To bond plastics, the use of adhesives and hot pressing have been proposed. In recent years, Aizawa has developed a CO₂-assisted polymer compression (CAPC) method, in which plastic fibers are attached by pressing in the presence of CO₂ at room temperature [6]. The protocol of this method is that the polymer is impregnated with CO₂, plasticized, and compressed. CO₂ is known to be easily soluble in polymers [7–9] and cause a decrease in the glass transition point and melting point [10–12]. Because CO₂ impregnation does not lower the glass transition point to room temperature, it is possible

to plasticize certain polymers to such a degree that they can be compressed. CAPC is a very convenient method of fabricating porous polymer materials because it can be conducted at room temperature, uses only CO₂, and achieves adhesion without using an adhesive. CO₂ is released from the fabricated material into the atmosphere to yield an uncontaminated porous body. Moreover, it is possible to control the porosity and pore size distribution by controlling the compression process [13]. The absence of heat and contamination in the process is expected to be most suitable for medicine, especially because the drug-containing sample will not undergo heat denaturation.

An application of plastics in the medical field is drug loading, which uses a water-absorbent polymer and various kinds of tapes such as poultice and bandage [14]. Recently, drug delivery has been extremely important to increasing the added value of a medicine [15]; it is a technique for delivering a designated medicine to a specified location, as well as for continuously supplying a specified medicine in a specified amount. Regarding the loading of the drug on a porous material, control of sustained release is expected because of the nature of the material [16–18].

CAPC enables a drug to be easily placed inside a porous material, and when the sample is used as medicine, control of sustained release is expected. This possibility is suggested by the controllability of porosity and pore size, although there have been no reports actually verifying this. In this study, we performed a quantitative analysis of the properties of sustained release of a drug, specifically methylene blue, from samples prepared using nonwoven fabrics.

Methylene blue has extremely low toxicity and is used as a fungicide in aquariums where tropical fish are bred [19–21]. If the tablet can gradually supply methylene blue to an aquarium, it would be possible to leave the tablet in a filter when the fish becomes sick. Therefore, using methylene blue for evaluation is meaningful from the point of view of further application.

First, we investigated the effect of thickness on the elution rate by using samples with different thickness but with the same porosity. Subsequently, the influence of porosity on the elution rate was investigated by fixing the thickness and varying the porosity. Finally, the effect of temperature on the elution rate was investigated by performing the experiment at temperatures between 10 and 60 °C. For these set of experiments, the elution rate was analyzed using a diffusion model, and the influences of the porosity and tortuosity on the diffusion rate in the porous material were discussed.

2. Materials and Methods

2.1. Preparation of Drug-Containing Samples

Methylene blue (CAS No. 7220-79-3) was purchased from FUJIFILM Wako Pure Chemical Co. (Osaka, Japan) and used without further purification. The nonwoven fabric (basis weight: about 30 g m⁻², average diameter: 8 μm) was manufactured by Nippon Nozzle Co., Ltd. (Kobe, Japan) through a melt-blown method using polyethylene terephthalate (PET) pellets (density: 1.34 g mL⁻¹, Bell Polyester Products Inc., Product name: TK3, Yamaguchi, Japan). Samples with diameters of 18 or 8 mm were punched out from the fabric.

Figure 1 shows the diagram of the cross-section of the high-pressure vessel used to prepare samples via CAPC and the tube connections. The drug-containing sample was prepared by placing a 8-mm round nonwoven fabric on a polytetrafluoroethylene (PTFE) sheet and dropping 10 μL of a 2 wt % solution of methylene blue (in 1:3 ethanol/water). The fabric was then dried and enclosed inside a tablet. The upper left corner of Figure 1 shows the nonwoven fabrics used in the CAPC process. The methylene-blue-loaded fabric (upper middle) was placed inside the 9-mm hole of the donut-shaped nonwoven fabric (lower middle). The top and bottom of this fabric were sealed with the nonwoven fabrics shown on the lower left and right corners of the image. After combining all sheets, the sample underwent CAPC treatment.

In the CAPC process, the piston (P) was first lowered to a certain distance from the bottom of the pressure vessel (B2). CO₂ was introduced by vapor pressure at a position 1.5 times higher than the press position. The piston and pressure vessel were sealed with the O ring provided on the side of the

piston. Because the CO₂ cylinder (C) connected to the pressure vessel was below the position of the O ring, the CO₂ introduced into the pressure vessel struck the piston and was supplied to the sample through the gap between the piston and pressure vessel. Subsequently, the introduction and discharge of CO₂ were repeated three times before replacing air with CO₂. The piston was lowered to the press position and the sample were pressed for 10 s. After the vessel was evacuated by opening the exhaust valve (V2), the piston was raised and the sample taken out. Because the CAPC process compressed the sheets at the press position, the thickness of the fabricated porous material was almost equal to this position.

Experiments were carried out to evaluate the effect of the diffusion distance using samples with the same porosity but different thicknesses. The effect of porosity dependence of elution was investigated by varying the number of the laminated sheets in the sample.

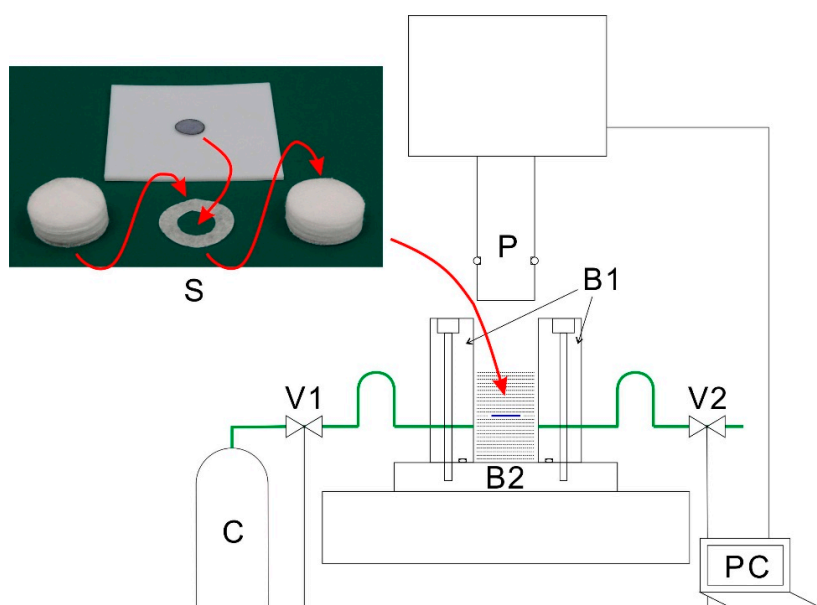


Figure 1. Schematic illustration of the cross-section of the high-pressure vessel used for CO₂-assisted polymer compression. B1: Body of the high-pressure vessel, B2: Base of the high-pressure vessel, C: CO₂ cylinder, P: Piston, PC: Laptop computer, S: Sample, V1: Intake valve, and V2: Exhaust valve.

2.2. Porosity Evaluation

Porosity was evaluated in terms of polymer density, weight of the fabric sheet, and sample thickness. The datasheet for the PET pellet indicated that the density of the used polymer is 1.34 g mL⁻¹. For a solid without a void, the thickness can be easily calculated using the weight, density, and diameter of the fabric sheet. The thickness at the center of the drug-containing sample was measured using a micrometer screw gauge. Assuming that the center of the drug-loaded nonwoven fabric was also compressed like the sides of the fabric, the thickness of one sheet can be estimated by dividing the measured thickness by the number of nonwoven fabrics. The difference between the thickness of the solid (L_{solid}) and actual thickness (L_{sample}) was considered as the total area of the pore, and the porosity α was calculated as $\alpha = (L_{\text{sample}} - L_{\text{solid}})/L_{\text{sample}}$.

2.3. Elution Rate Measurement

In the elution test, the sample was immersed in water, and the amount of methylene blue eluted in water was measured as concentration change by UV/visible spectroscopy (Shimadzu Co., Kyoto, Japan). The sample holder and experimental set-up are described in Figure 2. The sample holder was made of PTFE to avoid adsorption, and was originally designed by computer numerical

control machining. The sample was held in a hole in the sample holder and its outer periphery was sandwiched and fixed with a PTFE clip.

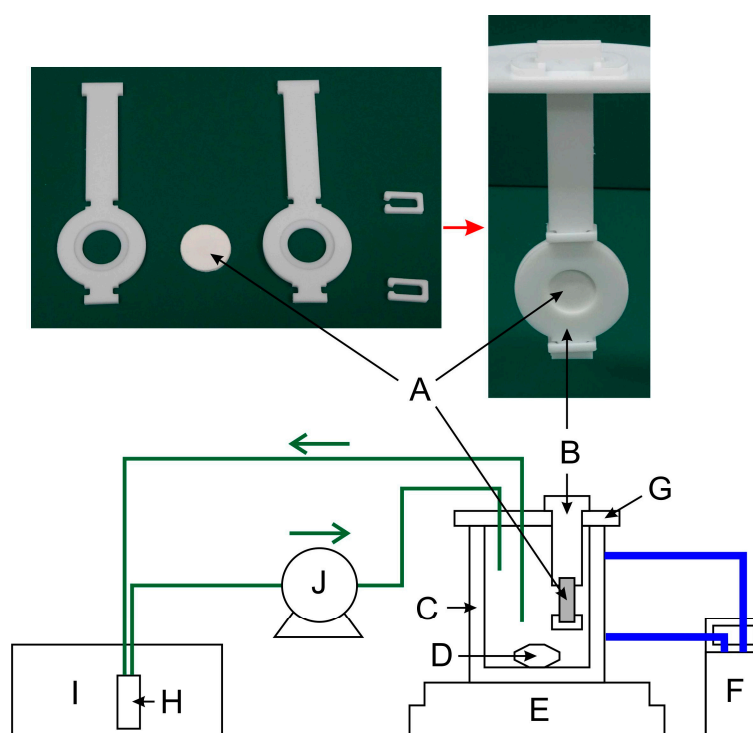


Figure 2. Schematic illustration of the set-up for drug release evaluation. A: Sample, B: Sample holder, C: Jacketed beaker, D: Stirrer bar, E: Magnetic stirrer, F: Circulating water bath, G: Beaker cap, H: Quartz flow cell, I: UV/vis spectrophotometer, and J: Peristaltic pump.

2-Morpholinoethanesulfonic acid (MES) monohydrate (CAS No. 145224-94-8) was purchased from Dojindo Laboratories (Kamimashikigun, Japan) and used without further purification. The MES buffer solution (1 mM, pH 6.2) was prepared using water purified by ion exchange and distillation. Two hundred milliliters of this solution was placed in a thermostatic jacketed beaker (C). The temperature was adjusted to the specified temperature by a circulating thermostatic water bath (F). The beaker containing the sample holder was confirmed to reach the desired temperature in about 10 min; thus, after more than 1 h, the sample was set in the sample holder and measurement was initiated (defined as time 0). The liquid inside the beaker was stirred at 200 rpm using a magnetic stirrer (E) and circulated to a flow cell (optical path length: 1 cm) at a flow rate of 8.8 mL h^{-1} using a peristaltic pump (J). A low setting was used for the magnetic stirrer to prevent flow inside the drug-containing sample. The flow cell (H) was a commercially available branch-type flow cell for the UV/vis spectrophotometer. The absorbance ($\lambda = 664 \text{ nm}$) of the methylene blue eluted in the aqueous phase was measured at 5-min intervals using a UV/vis spectrophotometer (Shimadzu UV-3150, Kyoto, Japan).

2.4. Estimation of Solubility

An excess amount of methylene blue was added to an aqueous solution containing 1 mM MES buffer and stirred in a water bath at $25 \text{ }^\circ\text{C}$. An aliquot of 0.5-mL was taken and centrifuged using a centrifugal filter unit (Durapore PVDF, $0.1 \text{ }\mu\text{m}$, Merck Millipore, Darmstadt, Germany) at 2000 rpm to achieve solid-liquid separation. The liquid phase was diluted 10,000 times; then, the absorbance at 664 nm was measured using a UV/vis spectrophotometer. As a result, the absorbance was almost stabilized after about 2 h. Therefore, after stirring the liquid for more than 12 h under different temperature conditions, visible absorption was similarly measured to evaluate saturation solubility.

3. Results and Discussion

First, validation of the concentration measurement and calibration of the absorbance against concentration were carried out. The observed spectra of methylene blue in the MES buffer solution at steady-state condition are shown in Figure 3a. The linear relationship between the absorbance at 664 nm and methylene blue concentration was maintained up to a concentration of 12 μM (Figure 3b).

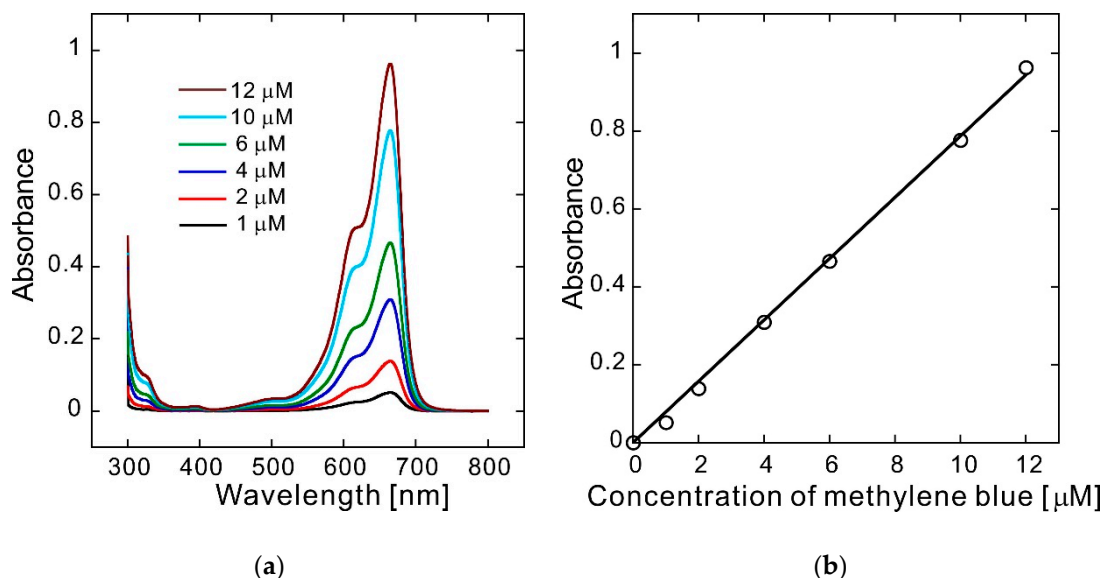


Figure 3. (a) UV/vis absorbance spectra of methylene blue and (b) absorbance at 664 nm as a function of concentration.

The correlation between elution distance and elution rate was investigated using samples prepared by changing the number of sheets and sample thickness simultaneously to obtain similar porosities. The absorbance is converted to solution concentration, C_{bulk} , which is fitted to an exponential increase equation (Figure 4). The range of the best-fit line (solid line) is the range of the fitted data, which matches the experimental results well. The fitting equation is as follows:

$$C_{\text{bulk}} = m_1(1 - \exp(-m_2 \times (t - m_3))) \quad (1)$$

where m_1 is the equilibrium concentration, m_2 is the apparent elution rate, m_3 is the apparent delay time, and t is the time. The delay time is the time taken by the buffer solution to penetrate the sample and reach the methylene-blue-loaded fabric and for methylene blue to diffuse from the sample.

Because methylene blue did not remain in the sample after the elution test, it was assumed that all of it diffused into the bulk. This suggests that there is no special interaction between methylene blue and the nonwoven fabric.

C_{bulk} rises exponentially at rate m_2 after a certain time m_3 and eventually approaches m_1 . As the number of sheets n increases and the elution distance lengthens, m_2 becomes slower (Table 1). Although the samples were prepared similarly, there is a slight variation in m_1 . This is because while methylene blue is placed on the nonwoven fabric, part of it remains on the PTFE sheet (Figure 1) depending on the sample, leading to a difference in the amount of methylene blue loaded.

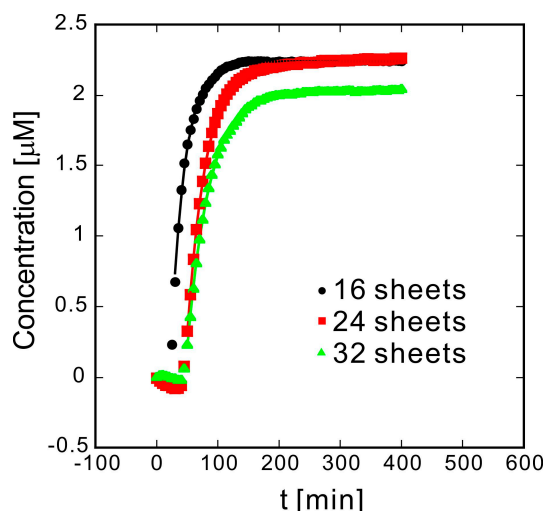


Figure 4. Time dependence of methylene blue absorbance at 664 nm for different quantities of laminated sheets. The markers indicate experimental results, and the solid line is the result of fitting the experimental data to the exponential function ($m_1 \times (1 - e^{(-m_2 \times (t-m_3))})$) using the least squares method.

Table 1. Thickness δ and porosity α of samples with n sheets and related parameters ¹ of methylene blue elution.

ID	n	Weight of n Sheets (g)	δ (mm)	α	m_1 (μM)	m_2 (min^{-1})	m_3 (min)
a	16	0.124	1.331	0.436	2.24	0.0443	21.0
b	24	0.186	2.015	0.447	2.25	0.0323	45.3
c	32	0.248	2.701	0.453	2.09	0.0272	45.9

¹ m_1 , equilibrium concentration; m_2 , apparent elution rate; m_3 , apparent delay time.

In this experiment, samples are slowly circulated between the beaker and optical cell by the peristaltic pump (8.8 mL h^{-1}), and a time difference occurs between the change in concentration in the beaker and reflection for the optical cell. Therefore, the time constant of the experimental set-up was estimated. After methylene blue was dropped in the beaker, the time dependence of the absorbance was measured with the dropping time set to 0, and the response of the optical cell due to the instantaneous rise of the concentration in the beaker, as well as an exponential rise in delay time, was observed. The delay time at this time was $m_3' = 6.73 \text{ min}$ and elution rate m_2' was 0.1623 min^{-1} . When both the behavior of elution and observed reflection are exponential, there is a difference between the true elution rate, m_2'' , and m_2' , and true delay time, m_3'' , and m_3' . The differences are described as follows:

$$m_2 = \frac{m_2' m_2''}{m_2' + m_2''} \tag{2}$$

$$m_3 = m_3' + m_3'' \tag{3}$$

When the observed delay time is short ($m_3' \ll m_3''$) and the reflection rate is high ($m_2' \gg m_2''$), m_3'' and m_3 , and m_2'' and m_2 are in agreement. However, in this experiment, these conditions were not satisfied. Thus, it was necessary to calculate m_2'' and m_3'' from Equations (4) and (5).

$$m_2'' = \frac{m_2 m_2'}{m_2' - m_2} \tag{4}$$

$$m_3'' = m_3 - m_3' \tag{5}$$

The plot of the derived values in Figure 5 show that m_2'' decreases as δ increases.

The effective diffusion coefficient in the porous material (D_{eff}) of the tablet was investigated by constructing a diffusion model. In this model, the state after delay time m_3'' associated with the initial penetration of water, as seen in the experiment, was set to time 0. In addition, to simplify the model, unidirectional diffusion behavior in a porous material with an area twice the elution cross-section was assumed instead of gradual release of the drug at the center from both sides of the tablet (Figure 6). The thickness of the diffusion layer (L) was calculated from the number of sheets (n) on each side, total number of sheets ($2n + 1$), and sample thickness δ , assuming that the overlapping nonwoven fabrics are evenly compressed (Figure 6).

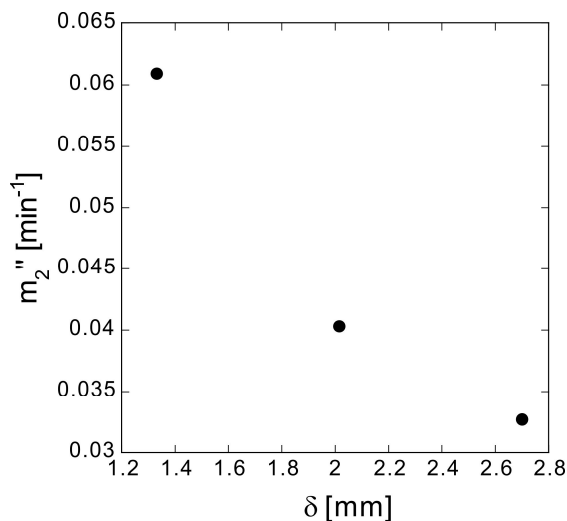


Figure 5. True elution rate constant m_2'' at different sample thicknesses δ .

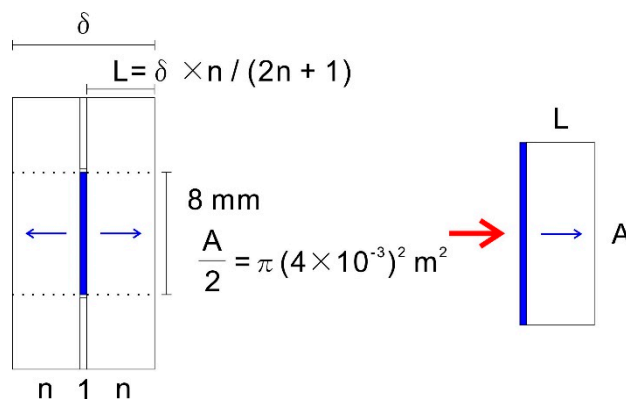


Figure 6. Diffusion model for the release of the drug from the tablet.

The driving force for the diffusion of solute in solution is the concentration difference, and in describing the diffusion behavior in the tablet, estimation of the concentration inside the tablet (C_{drug}) is indispensable. Experimental results showed that the concentration outside the tablet is C_{bulk} , which is 0 at time 0 and m_1 at time ∞ . As shown above, C_{bulk} rose exponentially. On the basis of this information, we attempted to formulate a model. First, it was assumed that C_{drug} at time 0, which is unknown, is C_0 . At time ∞ , C_{drug} coincides with C_{bulk} , and the release of the drug, with concentration as the driving force, stops. When the amount of solute introduced into the porous material and the amount of solute discharged from the porous material are equivalent, the decay of C_{drug} should be exponential, since the change in C_{bulk} after passing through the porous material is also exponential. Thus, it is necessary to link $C_{drug}(0) = C_0$ and $C_{drug}(\infty) = m_1$ exponentially. Then, under the condition that the amount of solute introduced into the porous material is equal to the amount of solute discharged from

the porous material, the rate constant for the decrease in C_{drug} must match the rate constant for the increase in C_{bulk} . Based on this hypothesis, the following equation was derived:

$$C_{drug} = m_1 + (C_0 - m_1) \exp(-m_2'' t) \quad (6)$$

Table 2 summarizes the concentration difference between the interior of the tablet and the bulk, which is the driving force for diffusion.

Table 2. Concentrations inside (C_{drug}) and outside (C_{bulk}) the tablet at different times.

Time	C_{drug} ¹	C_{bulk}
0	C_0	0
t	$m_1 + (C_0 - m_1) \exp(-m_2'' t)$	$m_1(1 - \exp(-m_2'' t))$
∞	m_1	m_1

¹ C_0 , concentration at $t = 0$; m_1 , equilibrium concentration; m_2'' , true elution rate constant.

The change in diffusion flow rate J was calculated from the amount of solute eluted from the tablet. If the bulk amount of water is V_{bulk} and the pores in the tablet are V_{void} , the bulk amount of water after the water has seeped into the pores is $(V_{bulk} - V_{void})$. Sample c in Table 1 has the largest V_{void} among the samples; V_{void} is about 0.3 mL ($0.9 \times 0.9 \times 3.14 \times 0.2701 \times 0.453$), which is negligible compared to V_{bulk} in the beaker (200 mL). That is, the space inside the tablet is very small relative to V_{bulk} ($V_{bulk} \gg V_{void}$); thus, in this experiment, V_{bulk} can be considered constant at 200 mL. Under this condition, by multiplying the C_{bulk} (mol m^{-3}) by V_{bulk} ($200 \text{ mL} = 2 \times 10^{-4} \text{ m}^3$), the amount of methylene blue eluted from the tablet into bulk water can be obtained. Under the condition that the concentration gradient in the porous material can be approximated linearly, J is given by

$$J = \frac{D_{eff}(C_{drug} - C_{bulk})}{L} = \frac{D_{eff}C_0 \exp(-m_2'' t)}{L} \quad (7)$$

Thus, D_{eff} can be calculated using the equation

$$D_{eff} = \frac{L J}{C_0 \exp(-m_2'' t)} \quad (8)$$

On the other hand, since the elution rate is obtained by differentiating the amount eluted into bulk water ($2 \times 10^{-4} C_{bulk}$) by t , J is given by

$$J = \frac{2 \times 10^{-4} m_1 m_2'' \exp(-m_2'' t)}{A} \quad (9)$$

From Equations (8) and (9), D_{eff} is derived as follows:

$$D_{eff} = \frac{2 \times 10^{-4} m_1 m_2'' L}{A C_0} \quad (10)$$

Normally, since the unit of D_{eff} is $\text{m}^2 \text{ s}^{-1}$, it is necessary to convert the units of m_1 to mol m^{-3} , m_2'' to s^{-1} , L to m , A to m^2 , and C_0 to mol m^{-3} . Usually, elution from solid drugs is indicated by elution of the surface of the drug into the solvent and diffusion after elution. For the concentration near the surface of the drug, the saturation solubility should be used as C_0 . The solubility S was determined using a van't Hoff plot with $1/T$ on the abscissa and $\ln S$ on the ordinate. In Figure 7, the markers are the measured values and the solid line is the linear fitting obtained by the least squares method. To suppress fluctuations in the experiments, subsequent analysis was performed using the S

obtained from the fitting of the van't Hoff plot. Data fitting using the least squares method yields the following equation:

$$\ln S = 12.49 - \frac{4394}{T} \tag{11}$$

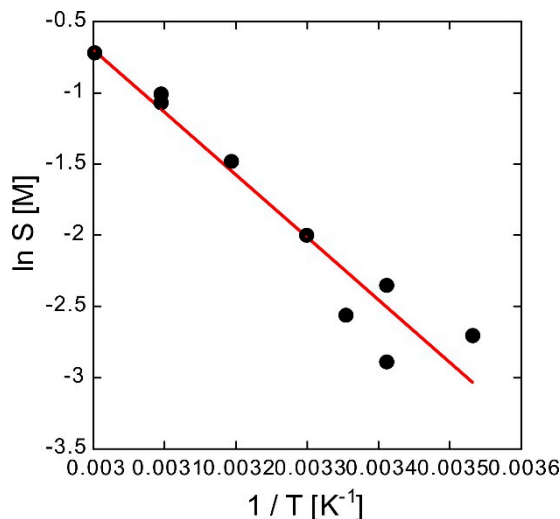


Figure 7. Van't Hoff plot of solubility *S* of methylene blue in 1 mM MES buffer solution.

The *S* in the aqueous solution containing 1 mM MES buffer at 25 °C, calculated from Equation (11), was 0.105 M. This is close to the solubility in water at 25 °C stated in the SDS sheet of the methylene blue reagent, which is 0.136 M.

The results of the calculation of *D_{eff}* in the porous body are shown in Table 3. It is known that *D_{eff}* in a porous body filled with solvent is smaller than the bulk diffusion coefficient. This is because the diffusion path is narrower if the solvent exists only in the gap of the porous material (effect of porosity). Furthermore, the path in the gap of the porous body is bent and the diffusion path is longer than *L* (effect of tortuosity). Assuming that the bulk diffusion coefficient is *D_{bulk}*, *D_{eff}* is given by the following equation [22].

$$D_{eff} = \frac{\alpha}{\tau} D_{bulk} \tag{12}$$

where τ is the tortuosity factor. For one-dimensional diffusion, τ is defined as the square of *L_{eff}*/*L*, where *L_{eff}* is the actual diffusion distance. The diffusion coefficient of methylene blue in water at 23 °C is $4.6 \times 10^{-10} \text{ m}^2 \text{ s}^{-1}$ according to Miložič et al. [23]. The arbitrary temperature can be estimated in proportion to the absolute temperature using the Einstein-Stokes equation. *D_{bulk}* at 25 °C is $4.6 \times 10^{-10} \text{ m}^2 \text{ s}^{-1}$, and the calculated τ values using this and Equation (12) are shown in Table 3. The *D_{eff}* and τ values of samples a, b, and c are same; thus, the decrease in *m₂*'' with increasing δ is caused by the expansion of the diffusion distance.

Table 3. Effective diffusion coefficient *D_{eff}* and tortuosity factor τ of samples and related parameters¹ of methylene blue elution.

ID	δ (mm)	α	<i>m₂</i> '' (min ⁻¹)	<i>m₃</i> '' (min)	<i>D_{eff}</i> (m ² s ⁻¹)	τ	<i>L_{eff}</i> / <i>L</i>
a	1.331	0.436	0.0609	14.3	2.8×10^{-11}	7.3	2.7
b	2.015	0.447	0.0403	38.6	2.8×10^{-11}	7.3	2.7
c	2.701	0.453	0.0327	39.2	2.9×10^{-11}	7.3	2.7

¹ δ , sample thickness; α , porosity; *m₂*'', true elution rate constant; *m₃*'', true delay time; *L*, thickness of diffusion layer; *L_{eff}*, actual diffusion distance.

Subsequently, without changing δ , samples with different compression ratios and associated α were produced by increasing the number of overlapping sheets. From samples a to g in Table 4, the number of sheets on one side (n) increases by two and α decreases. m_2'' increases as α increases (Figure 8) and since δ is almost the same, D_{eff} also decreases (Table 4). The calculated τ values of samples a, d, e, and f are almost the same, but that of sample g is higher; this may be due to the influence of sample fluctuation. It is natural that α decreases as the compression ratio increases and that τ shows a tendency to increase. Nevertheless, the difference in D_{eff} is considerably larger than the difference in τ , and the former is dominated by the decrease in the volume involved in elution caused by the decrease in α .

Table 4. Effect of compression ratio on parameters ¹ of methylene blue elution.

ID	n	Weight of n Sheets (g)	δ (mm)	α	m_2'' (min ⁻¹)	D_{eff} (m ² s ⁻¹)	τ	L_{eff}/L
a	16	0.124	1.331	0.436	0.0609	2.8×10^{-11}	7.3	2.7
d	18	0.140	1.333	0.367	0.0531	2.3×10^{-11}	7.3	2.7
e	20	0.155	1.333	0.301	0.0451	2.0×10^{-11}	7.1	2.7
f	22	0.171	1.335	0.231	0.0343	1.6×10^{-11}	6.7	2.6
g	24	0.180	1.335	0.165	0.0228	8.4×10^{-12}	9.1	3.0

¹ δ , sample thickness; α , porosity; m_2'' , true elution rate; D_{eff} , effective diffusion coefficient; τ , tortuosity factor; L , thickness of diffusion layer; L_{eff} , actual diffusion distance.

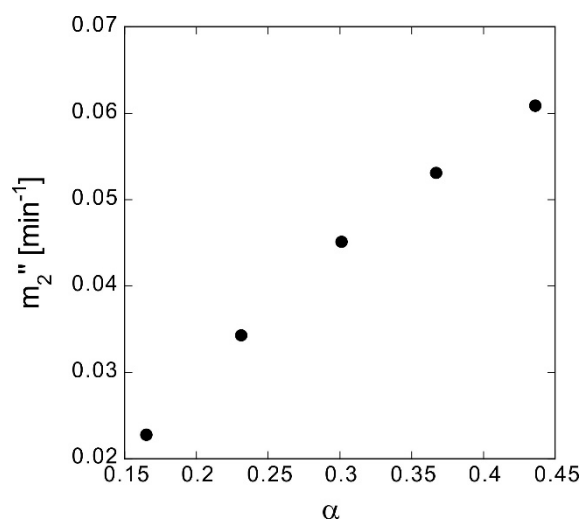


Figure 8. True elution rate m_2'' at different porosities α .

Finally, the temperature dependence of m_2'' was measured. The m_2'' values of samples h to m, prepared with 20 sheets pressed on one side, were measured from 10 to 60 °C. If the diffusion coefficient follows the Einstein-Stokes equation, it is proportional to the absolute temperature; however, the temperature dependence of m_2'' is not proportional to the absolute temperature (Figure 9). Thus, factors other than the diffusion coefficient should dominate the trend observed for m_2'' . Analysis based on the tablet elution model was consequently carried out.

Figure 10 shows that D_{eff} gradually increases with T . According to the Einstein-Stokes equation, D_{bulk} is proportional to T . For a porous material with the same α and degree of flexion, D_{eff} should also be proportional to T ; thus, the solid line from the least squares approximation shows proportionality. Although the data fluctuation is large, the trends generally agree. m_2'' varies significantly with T despite the moderate change in D_{eff} . This is because the S of methylene blue varies significantly with T (Table 5). With the concentration difference as the driving force, J increases, leading to an increase in m_2'' .

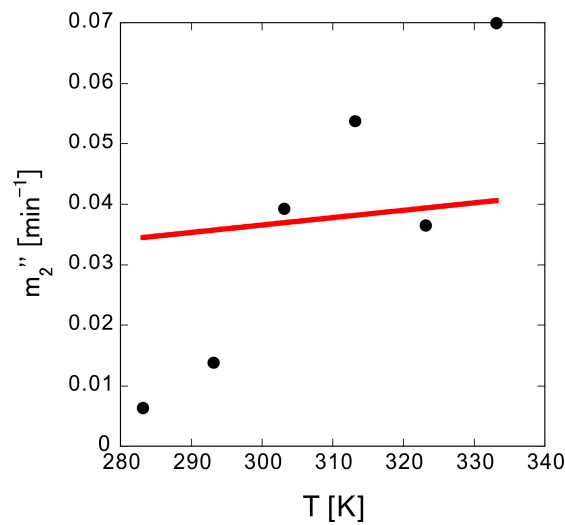


Figure 9. Temperature dependence of true elution rate m_2'' . The circles are experimental data, while the red solid line is the proportional fitting.

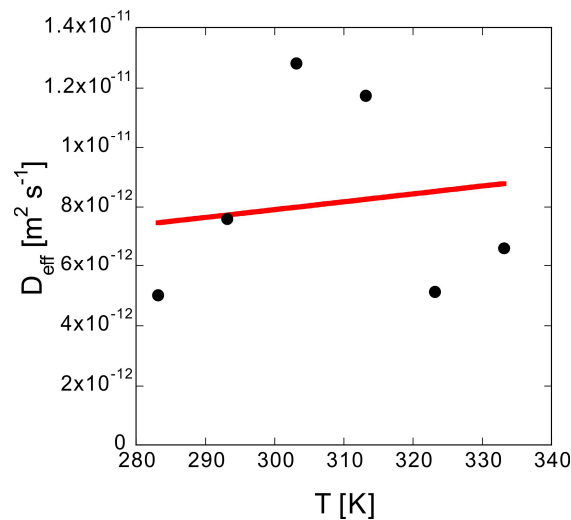


Figure 10. Temperature dependence of D_{eff} . The circles are experimental data, while the red solid line is the proportional fitting.

Table 5. Effect of temperature on parameters ¹ of methylene blue elution.

ID	T (°C)	Weight of n Sheets (g)	δ (mm)	α	m_2'' (min^{-1})	S (M)	D_{bulk} ($\text{m}^2 \text{s}^{-1}$)	D_{eff} ($\text{m}^2 \text{s}^{-1}$)	τ	L_{eff}/L
h	10	0.155	1.130	0.170	0.00604	0.048	4.4×10^{-10}	5.0×10^{-12}	15	3.9
i	20	0.155	1.132	0.171	0.0127	0.082	4.6×10^{-10}	7.6×10^{-12}	10	3.2
j	30	0.155	1.133	0.172	0.0316	0.13	4.7×10^{-10}	1.3×10^{-11}	6.3	2.5
k	40	0.155	1.128	0.168	0.0404	0.21	4.9×10^{-10}	1.2×10^{-11}	7.0	2.6
l	50	0.155	1.129	0.169	0.0298	0.33	5.0×10^{-10}	5.1×10^{-12}	17	4.1
m	60	0.155	1.131	0.170	0.0489	0.94	5.2×10^{-10}	6.6×10^{-12}	13	3.6

¹ δ , sample thickness; α , porosity; m_2'' , true elution rate constant; S, solubility; D_{bulk} , diffusion coefficient in bulk water; D_{eff} , effective diffusion coefficient; τ , tortuosity factor; L, thickness of diffusion layer; L_{eff} , actual diffusion distance.

4. Conclusions

In this study, various drug-containing tablets were prepared and their controlled release was analyzed by determining the effects of thickness, porosity, and temperature. A diffusion model that assumes an exponential decrease in the drug concentration inside the tablet from the saturated solubility was formulated. The drug placed inside the nonwoven fabric would diffuse through various

paths from the interior to the surface. When medicine carried on a nonwoven fabric is used as a drug supply, it is assumed that the drug on the surface would be released earlier, while that inside would be gradually released. The drug inside goes through the nonwoven fabric and reaches the surface, and this can be considered an exponential decrease in the drug supply.

The proposed diffusion model of the drug-loaded tablet explained the experimental data well. The experiments showed that thickness and porosity significantly affected sustained release performance. Using the model to calculate the effective diffusion coefficient and tortuosity factor showed that a decrease in porosity did not significantly increase the tortuosity factor. In the experiments, the decrease in the diffusion volume was the dominant factor in the change in the effective diffusion coefficient of the porous material.

We verified that the model can predict the sustained release rate through fitting experiment data for the elution behavior. The effective diffusion coefficient can be calculated from the sustained release rate; conversely, when the effective diffusion coefficient of a sample is known, the sustained release rate can be calculated using the model. In other words, it is possible to use the proposed diffusion model to design tablets that can realize a specific sustained release rate.

Author Contributions: T.A. conceived and designed the experiments; T.A. and Y.W. performed the experiments; T.A. and Y.W. analyzed the data; T.A. wrote the paper.

Funding: This research received no external funding.

Conflicts of Interest: The authors declare no conflict of interest.

References

1. Young, R.J.; Lovell, P.A. *Introduction to Polymers*, 3rd ed.; Routledge: Abingdon, UK, 2011; ISBN 978-0849339295.
2. Junqueira, M.V.; Bruschi, M.L. A review about the drug delivery from microsponges. *AAPS PharmSciTech* **2018**, *19*, 1501–1511. [[CrossRef](#)] [[PubMed](#)]
3. Okamoto, K.T. *Microcellular Processing*; Hanser Gardner Publications, Inc.: Cincinnati, OH, USA, 2003; ISBN 9781569903445.
4. Jacobs, L.J.M.; Kemmere, M.F.; Keurentjes, J.T.F. Sustainable polymer foaming using high pressure carbon dioxide: A review on fundamentals, processes and applications. *Green Chem.* **2008**, *10*, 731–738. [[CrossRef](#)]
5. Sauceau, M.; Fages, J.; Common, A.; Nikitine, C.; Rodier, E. New challenges in polymer foaming: A review of extrusion processes assisted by supercritical carbon dioxide. *Prog. Polym. Sci.* **2011**, *36*, 749–766. [[CrossRef](#)]
6. Aizawa, T. A new method for producing porous polymer materials using carbon dioxide and a piston. *J. Supercrit. Fluids* **2018**, *133*, 38–41. [[CrossRef](#)]
7. Li, M.; Huang, X.; Liu, H.; Liu, B.; Wu, Y.; Wang, L. Solubility prediction of supercritical carbon dioxide in 10 polymers using radial basis function artificial neural network based on chaotic self-adaptive particle swarm optimization and K-harmonic means. *RSC Adv.* **2015**, *5*, 45520–45527. [[CrossRef](#)]
8. Shieh, Y.-T.; Su, J.-H.; Manivannan, G.; Lee, P.H.C.; Sawan, S.P.; Spall, W.D. Interaction of supercritical carbon dioxide with polymers. I. Crystalline polymers. *J. Appl. Polym. Sci.* **1996**, *59*, 695–705. [[CrossRef](#)]
9. Shieh, Y.-T.; Su, J.-H.; Manivannan, G.; Lee, P.H.C.; Sawan, S.P.; Spall, W.D. Interaction of supercritical carbon dioxide with polymers. II. Amorphous polymers. *J. Appl. Polym. Sci.* **1996**, *59*, 707–717. [[CrossRef](#)]
10. Nalawade, S.P.; Picchioni, F.; Janssen, L.P.B.M. Supercritical carbon dioxide as a green solvent for processing polymer melts: Processing aspects and applications. *Prog. Polym. Sci.* **2006**, *31*, 19–43. [[CrossRef](#)]
11. Lian, Z.; Epstein, S.A.; Blenk, C.W.; Shine, A.D. Carbon dioxide-induced melting point depression of biodegradable semicrystalline polymers. *J. Supercrit. Fluids* **2006**, *39*, 107–117. [[CrossRef](#)]
12. Kikic, I. Polymer–supercritical fluid interactions. *J. Supercrit. Fluids* **2009**, *47*, 458–465. [[CrossRef](#)]
13. Aizawa, T. Fabrication of porosity-controlled polyethylene terephthalate porous materials using a CO₂-assisted polymer compression method. *RSC Adv.* **2018**, *8*, 3061–3068. [[CrossRef](#)]
14. Modjarrad, K.; Ebnesajjad, S. *Handbook of Polymer Applications in Medicine and Medical Devices*; Elsevier: Oxford, UK, 2014; ISBN 978-0323228053.

15. Wang, C.; Xu, P.; Zhang, L.; Huang, J.; Zhu, K.; Luo, C. Current strategies and applications for precision drug design. *Front. Pharmacol.* **2018**, *9*, 787. [[CrossRef](#)] [[PubMed](#)]
16. Lim, J.I.; Lee, W.K. Preparation of macroporous chitosan patch using co-solvent as a transdermal drug-delivery system. *J. Porous Mater.* **2014**, *21*, 783–788. [[CrossRef](#)]
17. Dastidar, D.G.; Saha, S.; Chowdhury, M. Porous microspheres: Synthesis, characterisation and applications in pharmaceutical & medical fields. *Int. J. Pharm.* **2018**, *548*, 34–48. [[CrossRef](#)]
18. Cheng, H.; Yang, X.; Che, X.; Yang, M.; Zhai, G. Biomedical application and controlled drug release of electrospun fibrous materials. *Mater. Sci. Eng.* **2018**, *90*, 750–763. [[CrossRef](#)] [[PubMed](#)]
19. Levine, G.; Meade, T.L. The effects of disease treatment on nitrification in closed system aquaculture. *J. World Aquac. Soc.* **1976**, *7*, 483–493. [[CrossRef](#)]
20. Tieman, D.M.; Goodwin, A.E. Treatments for ich infestations in channel catfish evaluated under static and flow-through water conditions. *N. Am. J. Aquac.* **2001**, *63*, 293–299. [[CrossRef](#)]
21. Sipos, A.J.; Urakawa, H. Differential responses of nitrifying archaea and bacteria to methylene blue toxicity. *Lett. Appl. Microbiol.* **2015**, *62*, 199–206. [[CrossRef](#)] [[PubMed](#)]
22. Epstein, N. On tortuosity and the tortuosity factor in flow and diffusion through porous media. *Chem. Eng. Sci.* **1989**, *44*, 777–779. [[CrossRef](#)]
23. Miložič, N.; Lubej, M.; Novak, U.; Žnidaršič-Plazl, P.; Plazl, I. Evaluation of diffusion coefficient determination using a microfluidic device. *Chem. Biochem. Eng. Q.* **2014**, *28*, 215–223. [[CrossRef](#)]



© 2018 by the authors. Licensee MDPI, Basel, Switzerland. This article is an open access article distributed under the terms and conditions of the Creative Commons Attribution (CC BY) license (<http://creativecommons.org/licenses/by/4.0/>).